

On the Continuum Limit of Topological Charge Density Distribution

P.Yu. Boyko, F.V. Gubarev,

*Institute of Theoretical and Experimental Physics,
B.Chermushkinskaya 25, Moscow, 117218, Russia*

Abstract

The bulk distribution of the topological charge density, constructed via HP^1 σ -model embedding method, is investigated. We show that the existence of quadratic power correction to gluon condensate implies linear divergence of the non-perturbatively defined topological density in the continuum limit. As a consequence, the topological charge is to be distributed within three-dimensional sign-coherent domains and conversely, the dimensionality of sign-coherent regions dictates the leading divergence of the topological density. Furthermore, we construct unambiguous definition of the dimensionality of relevant topological fluctuations. Confronting our findings with lattice data we obtain consistent qualitative picture of the topological density distribution in the continuum limit.

1 Introduction

Topology investigations had always been conspicuous topic for the lattice community and the recent advances indeed put it on the solid grounds. Both the topological charge and its density are now computable on thermalized vacuum configurations and the results already obtained in pure Yang-Mills theories indicate that the conventional instanton based models are to be strongly modified. Here we basically mean the discovery of global topological charge sign-coherent regions [1] and, what is even more important for us, the lower dimensionality of these regions [1, 2, 3, 4, 5], which are now believed to be three-dimensional. Note that the lower dimensionality of physically relevant vacuum fluctuations should not come completely unexpected, it had been repeatedly discussed in the recent past (see, e.g., Refs. [6, 7, 8]).

It is important that qualitatively the same picture of topological fluctuations appeared recently within radically different topology investigation approach introduced and developed in Refs. [9, 10]. Without mentioning all the details and technicalities involved we note only that the HP^1 embedding method is the nearest to the classical ADHM investigation of $SU(2)$ gauge fields topology and essentially reconstructs the topology defining map $S^4 \rightarrow HP^1 = S^4$, in terms of which both the topological charge and its density obtain unambiguous and well defined meaning. We are not in the position to review all the results obtained in [9, 10], however, it is important that HP^1 embedding allows to get rid of leading perturbative divergences in various observables. Moreover, it reproduces the topological aspects of $SU(2)$ Yang-Mills theory, is fairly compatible with other topology investigation approaches and allows to calculate with amazing accuracy the gluon condensate, demonstrating firmly that its quadratic power correction does not vanish. Starting just from observations and exploiting the geometrical clarity of HP^1 embedding approach we argue in section 2.1 that even the non-perturbatively defined topological density is to be linearly divergent in the continuum limit. This divergence implies in turn rather peculiar geometry of the relevant topological excitations. Namely, we show in section 2.2 that the topological charge sign-coherent regions are to be three-dimensional domains embedded into original four-dimensional space. The consistency check of this scenario is provided by the fluctuations of topological charges associated with sign-coherent regions.

Attempt to confront these findings with the lattice data brings out a wealth of both technical and theoretical issues, which we believe are adequately addressed in section 3. The measurements of the UV behavior of the topological density necessitates the invention of new calculation algorithm, which turns out to be fast and rather accurate. It allows us to make (sections 3.1, 3.2) statistically significant comparison of the theoretical considerations with lattice data and confirms that the characteristic topological density is indeed divergent, but at most linearly, in the continuum limit. As far as the dimensionality of relevant fluctuations is concerned, we investigate it in section 3.3 and develop unambiguous method of its determination, which involves, in fact, no one free parameter. Essentially it is the specially crafted biased random walk model embedded into the external environment dictated by the topological density¹. This approach allows us to show that indeed the density is concentrated in lower dimensional manifolds. Finally we investigate the fluctuations of the topological charges associated with sign-coherent regions

¹ During this paper preparation we learned that similar in spirit, but by no means identical to ours, ideas were discussed in Ref. [11].

and argue that only three-dimensional domains with linearly divergent topological density are consistent with theoretical and experimental restrictions imposed on the structure of topological fluctuations.

2 Scaling of Topological Density

In this section we analyze the topological charge density $q(x)$ obtained via recently developed [9, 10] HP^1 σ -model embedding method. The purpose is to show that the very existence of non-trivial quadratic correction to the gluon condensate, which is seen clearly in HP^1 projected fields, inevitably leads to the conclusion that the characteristic magnitude of non-perturbatively defined topological density is to be linearly divergent in the continuum limit. Moreover, the geometrical clarity of HP^1 embedding approach allows then to argue that the topological charge is to be concentrated in three-dimensional sign-coherent domains. The lower dimensionality of physically relevant fluctuations [6, 8] and, in particular, of the topological density distribution [1, 2, 3, 4] is the modern actively developing trend in the literature. However, as far as we can see our finding is the first theoretical derivation of this result. In fact, the argumentation could even be reversed, namely, the dimensionality of topological charge sign-coherent regions dictates the leading spacing dependence of the topological density. Finally, we show that the statistical distribution of the topological charges associated with sing-coherent regions provides the most stringent consistency check of our results.

2.1 Gluon Condensate, Leading Power Correction and Divergence of Topological Density

The essence of HP^1 σ -model embedding approach is the assignment of unique configuration of HP^1 σ -model fields $|q_x\rangle$ to every given $\text{SU}(2)$ gauge background A_μ (until section 3 we use continuum notations), where $|q_x\rangle$ is two-component, normalized $\langle q_x | q_x \rangle = 1$, quaternion-valued column vector (see Refs. [9, 10] for details). The relevant configuration $|q_x\rangle$ is singled out by the requirement that it provides the absolute minimum to the functional

$$F(A, q) = \int d^4x \text{Tr} (A_\mu + \langle q | \partial_\mu | q \rangle)^2 \quad (1)$$

for given (fixed) gauge potentials A_μ . Note that gauge covariance is maintained exactly since the σ -model target space HP^1 is the set of equivalence classes with respect to $|q_x\rangle \sim |q_x\rangle v_x$, $v_x \in \text{SU}(2)$. The uniqueness of the minimum of (1) and the factual absence of Gribov copies problem was discussed in length in Refs. [9, 10] and here we take it for granted. Therefore the embedded HP^1 σ -model fields $|q_x\rangle$ are unique (although non-local) functions of the original potentials. However, the advantage is that the gauge fields topology becomes explicit in terms of $|q_x\rangle$ variables. Indeed, the gauge invariant projectors $|q_x\rangle\langle q_x|$ provide the map of compactified physical space S^4 into the target space HP^1 , the degree of which is equal to the topological charge of the original gauge background. Furthermore, the local distinction of this map from trivial one is the uniquely defined measure of the topological charge density. One could say that the sole purpose of

HP¹ embedding method is to locally reconstruct the topology defining map $S^4 \rightarrow \text{HP}^1$, which allows to get essentially all the topological properties of the original background.

Then it is natural to consider the HP¹ projection

$$A_\mu \rightarrow A_\mu^{\text{HP}} \equiv -\langle q | \partial_\mu | q \rangle, \quad (2)$$

which replaces A_μ with its best possible approximation by σ -model induced potentials. The striking properties of the projected fields A_μ^{HP} were investigated in details in Ref. [10]. In particular, it was shown that A_μ^{HP} exactly reproduce the most of non-perturbative aspects of the original $SU(2)$ configurations, while containing no sign whatsoever of usual perturbative divergences. To the contrary, the kernel of the map (2) was shown to correspond to pure perturbation theory with identically trivial topology and vanishing string tension. Without mentioning all the aspects and properties of HP¹ projection (2) let us note that it allows to calculate with inaccessible so far accuracy the gluon condensate and its leading power correction. Indeed, the spacing dependence of HP¹ projected gauge curvature $F_{\mu\nu}^{\text{HP}}$ was found to be astonishingly well described by

$$\langle \frac{1}{2} \text{Tr}(F_{\mu\nu}^{\text{HP}})^2 \rangle = \frac{4\alpha_2}{a^2} + \frac{\pi^2}{6} \langle \frac{\alpha_s}{\pi} G^2 \rangle, \quad (3)$$

$$\alpha_2 = [61(3) \text{ MeV}]^2, \quad \langle \frac{\alpha_s}{\pi} G^2 \rangle = 0.0271(10) \text{ GeV}^4, \quad (4)$$

where a is the lattice spacing ($1/a$ serves as the UV cutoff). It is crucial that Eq. (3) does not contain any sign of usual perturbative contribution of order $O(a^{-4})$. Note that the value of α_2 coefficient turns out to be unexpectedly small, nevertheless it fits nicely into the known bounds on the magnitude of the quadratic correction term (see Ref. [12] for recent review). While the actual numbers quoted in (4) are not important for the present investigation, it is crucial that they both are definitely non-zero and therefore the spacing dependence of $\langle \text{Tr}(F_{\mu\nu}^{\text{HP}})^2 \rangle$ includes only $O(a^{-2})$ and $O(a^0)$ terms.

To analyze the consequences of Eq. (3) let us parametrize the physical space S^4 and the target space $\text{HP}^1 = S^4$ with stereographically projected coordinates x_μ and y_μ , $\mu = 0, \dots, 3$, and consider arbitrary non-degenerate point at which $\det[\partial y / \partial x] \neq 0$. The geometric clarity of HP¹ σ -model fields allows to conclude that the projected potentials A_μ^{HP} are given by

$$A_\mu^{\text{HP}} = J_\mu^\nu A_\nu^{\text{inst}}(y), \quad J_\nu^\mu = \frac{\partial y^\mu}{\partial x^\nu}, \quad (5)$$

where $A_\nu^{\text{inst}}(y)$ is the well known potential of classical BPST instanton solution with unit radius. The corresponding HP¹ projected curvature is

$$F_{\mu\nu}^{\text{HP}} = J_\mu^{\rho_1} J_\nu^{\rho_2} F_{\rho_1 \rho_2}^{\text{inst}}, \quad (6)$$

$$\frac{1}{2} \text{Tr}(F_{\mu\nu}^{\text{HP}})^2 \propto (\text{Tr } g^2)^2 - \text{Tr } g^2, \quad (7)$$

where we have introduced the metric $g^{\mu\nu} = (1 + y^2)^{-1} \cdot J_\lambda^\mu J_\lambda^\nu$ and skipped inessential numerical factor. Therefore the study of the projected curvature $\langle \frac{1}{2} \text{Tr}(F_{\mu\nu}^{\text{HP}})^2 \rangle$ is equivalent to the investigation of the metric g associated with the topology defining map $S^4 \rightarrow \text{HP}^1$. In term of strictly positive eigenvalues λ_μ of g , Eqs. (3) and (7) imply

$$\langle \frac{1}{2} \text{Tr}(F_{\mu\nu}^{\text{HP}})^2 \rangle = \frac{\Lambda_{QCD}^2}{a^2} + \Lambda_{QCD}^4 \propto \sum_{\mu \neq \nu} \langle \lambda_\mu \lambda_\nu \rangle, \quad (8)$$

where we have generically indicated the IR physical scale involved in Eq. (3) by Λ_{QCD} and explicitly kept all powers of lattice spacing. Since various eigenvalues λ_μ enter independently in r.h.s. of Eq. (8) it seems natural to assume that the corresponding averages factorize $\sum \langle \lambda_\mu \lambda_\nu \rangle = \sum \langle \lambda_\mu \rangle \langle \lambda_\nu \rangle$. Note that this does not spoil rotational invariance. Confronting now the dependence of both sides on UV and IR scales we conclude that the only solution of Eq. (8) is given by

$$\langle \lambda_0 \rangle \propto 1/a^2, \quad \langle \lambda_i \rangle \propto \Lambda_{QCD}^2, \quad i = 1, 2, 3, \quad (9)$$

where without loss of generality the singular $\propto 1/a^2$ behavior is ascribed to the first eigenvalue. The conclusion is that the very existence of quadratic correction to gluon condensate as is seen in HP^1 projected fields implies rather peculiar local structure of the topology defining map $S^4 \rightarrow HP^1$, namely, it is highly asymmetric on average. It is worth to note that the standard picture without quadratic correction term in (8) would imply $\langle \lambda_\mu \rangle \propto \Lambda_{QCD}^2$ meaning that the topological charge of order unit is gathered at large (of order Λ_{QCD}^{-1}) distances. The singular behavior of one eigenvalue $\langle \lambda_0 \rangle \propto 1/a^2$ signifies immediately that the topological susceptibility $\chi = \langle Q^2 \rangle / V$ is saturated on submanifolds with characteristic four-volume of order $a \cdot \Lambda_{QCD}^{-3}$. In other words the topological density is to be concentrated mostly in three-dimensional domains embedded into Euclidean four-dimensional space (we return to this problem in section 2.2).

The above results have rather dramatic consequences for the topological density $q(x) \sim \text{Tr } F\tilde{F}$, where \tilde{F} is dual field strength and we systematically omit inessential numerical factors. Since the averaged value $\langle q \rangle$ is zero trivially, let us consider

$$\langle q^2 \rangle \propto \langle \text{Tr}(F\tilde{F}) \text{Tr}(F\tilde{F}) \rangle. \quad (10)$$

However, the quantity $\langle q^2 \rangle$ could only be meaningful provided that we are able to separate carefully the perturbation theory contribution to it. Indeed, the correct field-theoretical way to define $\langle q^2 \rangle$ is to consider the topological charge density correlation function $\langle q_0 q_x \rangle$ at vanishing distances

$$\langle q^2 \rangle = \lim_{|x| \rightarrow 0} \langle q_0 q_x \rangle \propto \lim_{|x| \rightarrow 0} \langle \text{Tr}(F\tilde{F})_0 \text{Tr}(F\tilde{F})_x \rangle, \quad (11)$$

at which it is perturbatively dominated, $\langle q_0 q_x \rangle \sim -1/|x|^8$. The negative sign here is well known [13] and implies that $\langle q^2 \rangle > 0$ is, in fact, a pure contact term arising from the product of two operators $\text{Tr } F\tilde{F}$ at the same point. Hence the perturbative ambiguities make the value of $\langle q^2 \rangle$ undefined and usually it is fixed by the requirement $\chi = \int \langle q_0 q_x \rangle$.

However, it is crucial that the HP^1 embedding approach to the gauge fields topology is factually free of perturbative ambiguities. The best illustration is provided by Eq. (3) and in connection with topological density correlation function we discuss this in section 3.2. Therefore the topological density within HP^1 embedding approach, which in the continuum limit is given explicitly by $q \propto \text{Tr } F^{HP} \tilde{F}^{HP}$, is not plagued by perturbative uncertainties. Moreover, Eq. (6) together with well known properties of instanton solution implies that

$$q \propto \text{Tr } F^{HP} \tilde{F}^{HP} \propto \frac{\det J}{(1 + y^2)^2} = \pm \det^{1/2} g. \quad (12)$$

Hence for the characteristic magnitude of the topological density \bar{q} we have

$$\bar{q}^2 = \langle q^2 \rangle \propto \langle \det g \rangle = \langle \prod_{\mu} \lambda_{\mu} \rangle \sim \frac{\Lambda_{QCD}^6}{a^2}, \quad (13)$$

where Eq. (9) and the factorization hypothesis outlined above had been used. The conclusion is that even the non-perturbatively defined topological density is divergent in the continuum limit and this is the direct consequence of the existence of quadratic correction to the gluon condensate. Note however that this divergence is incomparable with usual perturbative one $\langle q^2 \rangle \sim 1/a^8$, which, in fact, is even non-integrable. Of course, it is understood that the very definition of the topological density is arbitrary to large extent (full derivative could always be added). However, the HP¹ embedding method is specified completely with no free parameters involved. Moreover, the corresponding topological density is definitely exempt from perturbative divergences and already for this reason its unusual scaling properties are worth to be investigated. In turn the spacing dependence (13) implies rather peculiar structure of vacuum topological fluctuations which we consider in the next section.

2.2 Dimensionality of Topological Fluctuations

The problem to be addressed in this section is the geometrical properties of vacuum topological fluctuations and in particular their dimensionality. First, let us note that generically any particular distribution of topological density in finite volume V could be divided unambiguously into the regions V_+ ($q_x > 0$) and V_- ($q_x < 0$) of sign-coherent topological charge so that the total charge is given by

$$Q = \int q = \int_{V_+} q + \int_{V_-} q \equiv Q_+ - Q_-, \quad (14)$$

where the relative sign of Q_+ , Q_- was made explicit in the last equality ($Q_- > 0$). Note that we do not assume that the regions V_+ , V_- are connected or have any other specific properties ($V_+ + V_- \neq V$, in particular). As far as the mean squared topological charge is concerned, the decomposition (14) implies

$$\langle Q^2 \rangle \propto \langle Q_+^2 \rangle - \langle Q_+ Q_- \rangle, \quad (15)$$

where we have generically assumed that $\langle Q_-^2 \rangle = \langle Q_+^2 \rangle$. In turn for the topological susceptibility, which is *a priori* postulated to be finite in the continuum limit, we have

$$\chi \propto \frac{\langle Q_+^2 \rangle - \langle Q_+ Q_- \rangle}{V} \sim \Lambda_{QCD}^4. \quad (16)$$

It terms of the characteristic magnitude of the topological density \bar{q} the last equation becomes

$$\bar{q}^2 \frac{\langle V_+^2 \rangle - \langle V_+ V_- \rangle}{V} \sim \Lambda_{QCD}^4. \quad (17)$$

Keeping in mind the ultraviolet divergence of \bar{q} , Eq. (13), we conclude that the independent fluctuations of the volumes V_+ , V_- are strictly prohibited. Instead the magnitudes of V_+ and V_- are to be fine tuned up to the order $O(a^2)$

$$\langle (V_+ - V_-)^2 \rangle \sim a^2 \Lambda_{QCD}^{-2} \cdot V, \quad (18)$$

since otherwise the topological susceptibility would diverge in the continuum limit. It is important that, contrary to the case of zero-point fluctuations, for non-perturbatively defined topological density there are no arguments which would guarantee the exact generic cancellation of divergent terms in the integral $Q = \int q$. In fact, the fine tuning assumption (18) is not new, similar in spirit observations were made already in the recent past (see, e.g., Refs. [5, 7, 8, 14]). However, it seems for us that the necessity to fine tune the Yang-Mills theory is unnatural and we would like to reformulate the problem so that explicit powers of lattice spacing do not appear. Indeed, Eq. (18) arises precisely because the volumes V_+ , V_- were assumed to be four-dimensional. Evidently the fine tuning requirement (18) is satisfied identically once we suppose that the topological density is distributed in three-dimensional domains $V_{\pm}^{(3)} = V_{\pm}/a$, which are allowed to fluctuate on the scale of Λ_{QCD}

$$\langle (V_+^{(3)} - V_-^{(3)})^2 \rangle \sim V/\Lambda_{QCD}^2. \quad (19)$$

Note that (19) is not the real solution, but rather the reformulation, of the fine tuning problem. Indeed, although the explicit spacing dependence is gone, the three-dimensional structure of topological fluctuations in D=4 YM theory is equivalent, in fact, to a sort of fine tuning.

In order to make the presentation more coherent, let us return to Eq. (15). We could easily bypass Eq. (18) assuming that the charges Q_{\pm} fluctuate independently

$$\langle Q_+ Q_- \rangle = \langle Q_+ \rangle \langle Q_- \rangle = \langle Q_+ \rangle^2. \quad (20)$$

Then Eq. (16) translates into

$$\frac{\langle Q_+^2 \rangle - \langle Q_+ \rangle^2}{V} \propto \frac{\langle Q_+ \rangle}{V} \sim \bar{q} \frac{\langle V_+ \rangle}{V} \sim \Lambda_{QCD}^4, \quad (21)$$

where the validity of central limit estimate

$$\langle Q_+^2 \rangle - \langle Q_+ \rangle^2 \propto \langle Q_+ \rangle \quad (22)$$

was supposed. The relation between ultraviolet behavior of characteristic topological density and the dimensionality of the corresponding fluctuations could then be given as follows. Assume that \bar{q} is of order $a^{-\alpha}$, the dimensionality of the topological fluctuations is D and denote the lattice volumes by V_{\pm}^{lat} . Then

$$\chi \propto \Lambda_{QCD}^4 \sim \bar{q} \frac{a^{4-D} a^D \langle V_+^{lat} \rangle}{a^4 V^{lat}} \sim a^{4-\alpha-D} \cdot \frac{\langle V_+ \rangle}{V} \quad (23)$$

and the relation between UV behavior of the characteristic topological density and the dimensionality of the relevant topological fluctuations follows

$$\bar{q} \sim a^{-\alpha}, \quad \dim[V_{\pm}] = 4 - \alpha. \quad (24)$$

β	a, fm	L_t	L_s	V^{phys}, fm^4	N^{conf}	N_q^{conf}
2.4000	0.1193(9)	16	16	13.3(4)	198	70
2.4273	0.1083(15)	16	12	3.8(2)	250	80
2.4500	0.0996(22)	14	14	3.8(2)	200	80
2.4750	0.0913(6)	16	16	4.6(1)	380	75
2.5000	0.0854(4)	18	16	3.92(7)	200	75
2.5550	0.0704(9)	20	20	3.9(2)	80	80
2.6000	0.0601(3)	28	28	8.0(2)	65	60

Table 1: Simulation parameters.

However, it is clear that the argumentation relies heavily on the assumption that the fluctuations of the topological charges Q_{\pm} obey Eq. (20) (as well as Eq. (22), which, however, seems to be less restrictive). *A priori* Eq. (20) is by no means evident and being confronted with experimental lattice data provides the most stringent test of the above scenario. Various experimental aspects of the problem are addressed in the next section. Here we note only that Eqs. (13), (20) imply the three-dimensional structure of vacuum topological fluctuations. Evidently, the reversed argumentation could also be given, namely, the dimensionality of sign-coherent topological charge fluctuations determines the leading ultraviolet behavior of characteristic topological density provided that Eq. (20) is valid. We stress that the essence of the above presentation is the factual absence of leading perturbative divergences in HP^1 projected fields and in the corresponding topological density. One could convince oneself that in the case of perturbatively dominated topological density $\bar{q} \sim a^{-4}$ exactly the assumption (18) (with a^2 replaced by a^4 on the r.h.s.) holds true, while Eq. (20) is violated and reads instead $\langle Q_+ Q_- \rangle = \langle Q_{\pm}^2 \rangle$. The conclusion is that Eqs. (20), (22) are indeed crucial to validate the lower dimensionality of the topological charge fluctuations.

3 Confronting with Lattice Data

In this section we describe in details the results of our numerical investigations of the scenario outlined above. In section 3.1 the topological density at various scales is considered; we show that even the simplest approach indeed qualitatively confirms the divergence of characteristic topological density in the continuum limit. Section 3.2 is devoted to the investigation of $\langle q_0 q_x \rangle$ correlation function from which we deduce the scaling law of the characteristic topological density. Finally in section 3.3 we propose new method, which allows to establish the dimensionality of topological fluctuations without any additional parameters involved.

The numerical measurements were performed on 7 sets (Table 1) of statistically independent $\text{SU}(2)$ gauge configurations generated with standard Wilson action. The most of configurations listed in Table 1 are the same as were used in Refs. [9, 10] (except for the set at $\beta = 2.555$). The last column in Table 1 represents the number of configurations on which we calculated the bulk topological charge density. Note that the number of analyzed configurations at each spacing is indeed rather large, which is due to the new algorithm used to evaluate the topological density and which is described in Appendix.

The lattice spacing values quoted in Table 1 were partially taken from Refs. [15] and fixed by the physical value of SU(2) string tension $\sqrt{\sigma} = 440$ MeV. Note that for $\beta = 2.4273$ and $\beta = 2.555$ the lattice spacings and corresponding rather conservative error estimates were obtained via interpolation in between the points quoted in [15].

3.1 Topological Fluctuations at Various Scales

As was repeatedly stressed in Refs. [9, 10] any discussion of the topological charge density within the lattice settings inevitably introduces a particular cutoff Λ_q on the magnitude of the density so that $q(x)$ is equated to zero if $|q(x)| < \Lambda_q$. Indeed, the most straightforward argument here is that in the numerical simulations the density is always known with finite accuracy. Thus the numerical precision provides the finest possible cutoff which in physical units evidently scales like $\Lambda_q \propto a^{-4}$. Moreover, the introduction of (often implicit) finite Λ_q is inherent to all studies of the gauge fields topology. For instance, the overlap-based topological density, which is given by the sum of Dirac eigenmodes ψ_λ contributions, is usually either restricted to lowest modes, $\lambda < \Lambda \propto \Lambda_{QCD}$, or is considered for all modes available on the lattice, $\lambda \lesssim 1/a$. Therefore the actual problem is not the presence of the cut Λ_q , it is introduced always. The physically meaningful question is the spacing dependence $\Lambda_q = \Lambda_q(a)$ and the above examples illustrate two extreme cases $\Lambda_q \propto a^{-4}$ and $\Lambda_q \propto \Lambda_{QCD}^4$.

It is crucial that the scaling law $\Lambda_q(a)$ could be taken at will and we're going to exploit this freedom to study the spacing dependence of the topological density. Indeed, if the characteristic topological density \bar{q} stays constant in physical units then the volume density of points at which $|q(x)| > \Lambda_q$,

$$\rho(\Lambda_q) = \frac{1}{V} \sum_x \begin{cases} 1, & |q(x)| > \Lambda_q \\ 0, & \text{otherwise} \end{cases}, \quad (25)$$

should also be lattice spacing independent for $\Lambda_q \propto \Lambda_{QCD}^4$. Note that the lattice units had been used in (25) and that $\rho(\Lambda_q)$ is dimensionless, positive, bounded $\rho(\Lambda_q) \leq 1$ quantity. On the hand, the divergence $\bar{q} \sim a^{-\alpha}$ would result in the divergent behavior $\rho(\Lambda_q) \sim a^{-\alpha}$ of the volume density² for physical cut $\Lambda_q \propto \Lambda_{QCD}^4$, while $\rho(\Lambda_q)$ is to be almost spacing independent for similarly divergent cut $\Lambda_q \propto \Lambda_{QCD}^4 \cdot (a \Lambda_{QCD})^{-\alpha}$. Therefore the most straightforward way to analyze the spacing dependence of the characteristic topological density is to tune the scaling law $\Lambda_q(a)$ until the volume density $\rho(\Lambda_q)$ becomes constant at various lattice resolutions.

Unfortunately, this approach does not allow to investigate the dependence $\bar{q}(a)$ precisely. Indeed, on the lattice we could only probe a finite set of scaling laws $\Lambda_q(a)$, moreover the corresponding estimates of $\rho(\Lambda_q)$ are always biased. However, it is crucial that the correct qualitative picture could easily be obtained this way. We performed the measurements of the volume density $\rho(\Lambda_q)$ at various lattice spacings using three different scaling laws

$$\Lambda_q^{(n)} \propto \Lambda_{QCD}^4 \cdot (a \Lambda_{QCD})^{-n}, \quad n = 0, \dots, 2, \quad (26)$$

² Note that in the numerical simulations the singularity should not be expected, the divergence is only seen for $\rho \ll 1$.

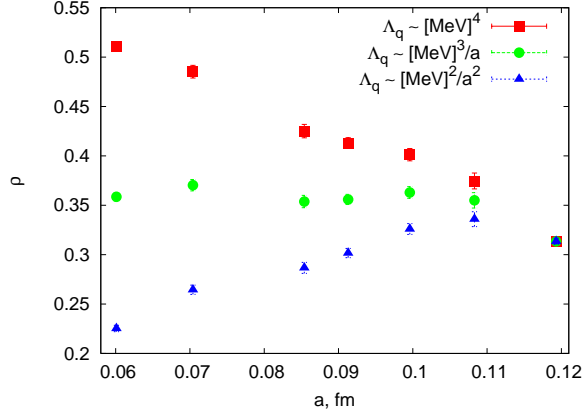


Figure 1: Volume density of points with $|q_x| > \Lambda_q$ as a function of lattice spacing at different Λ_q scaling laws (26).

where the numerical coefficients were chosen in such a way that $\Lambda_q^{(n)} = [200 \text{ MeV}]^4$, $n = 0, 1, 2$ at $a = 0.1193 \text{ fm}$. Note that the actual values of the cuts (26) in the whole range of lattice spacings considered are always below the lumps percolation transition ensuring that the cutoff Λ_q stays within the physically meaningful window (see Refs. [9, 10] for details). The results of our measurements are presented on Fig. 1 from which it is clear that the volume density of points with $|q_x| > \Lambda_q^{(0)} = [200 \text{ MeV}]^4$ is rapidly rising with diminishing lattice spacing. Contrary to that the linearly divergent cut on the topological density, $\Lambda_q^{(1)} \sim 1/a$ results in the almost spacing independent volume density $\rho(\Lambda_q^{(1)}) \approx 0.35$. On the other hand, once the quadratically divergent cut $\Lambda_q^{(2)} \sim 1/a^2$ is imposed the quantity $\rho(\Lambda_q^{(2)})$ diminishes almost linearly with vanishing lattice spacing and in the limit $a \rightarrow 0$ becomes compatible with zero. The conclusion is that the characteristic magnitude of the topological density is indeed singular in the continuum limit, the leading divergence is compatible with linear one

$$\bar{q} \propto \Lambda_{QCD}^3 / a \quad (27)$$

and is in accord with theoretical expectations (13).

Turn now to the consideration of the dimensionality of topological charge sign-coherent regions. Qualitatively the structure of topological fluctuations at various cuts Λ_q is rather simple [9, 10]. For utterly small values of Λ_q there are typically only two large (percolating) regions of sign-coherent topological density, each of which occupies almost half of the lattice volume and carries rather large topological charge Q_{\pm} , Eq. (14). With rising cutoff the volume density of percolating regions diminishes, while the number of small sign-coherent lumps rapidly grows. Finally a sort of percolation transition happens at which the percolating regions cease to exist and become indistinguishable from the small lumps. After that point the volume distribution of sign-coherent regions become universal (Λ_q independent) and is described by rather remarkable power law. However, the physics changes drastically at the lumps percolation transition. Namely, the string tension associated with the topology defining HP^1 projected fields and which account for the full $SU(2)$ string tension in the continuum limit vanishes. Already from this observation we expect that the most physically important topological fluctuations are represented by the largest

(at given cutoff Λ_q) lumps in topological density and it is natural to focus exclusively on their dimensionality.

However, at any fixed cutoff Λ_q the structure of the lumps is very complicated and their dimension is, in fact, not a well defined concept. Indeed, the notion of dimensionality makes sense only as a scaling relation since at any fixed lattice spacing the lumps occupy some finite fraction of the volume. Actually the situation is much worse since the very definition of the lumps require introduction of the cutoff Λ_q , the spacing dependence of which is not fixed. Moreover, admitting the lower dimensionality of sign-coherent regions, their volume fraction is not obliged to be finite in the continuum limit, hence even the spacing dependence of lumps localization degree (which might be expressed in terms of inverse participation ratio or similar quantities) would not reveal their dimensionality.

It is clear that the crucial obstacle in lumps dimensionality definition is the necessity to impose the cutoff on the topological density. The concept of the dimensionality of topological fluctuations would become unambiguous provided that we could get rid of explicit Λ_q and hence reject the language of the lumps. This program is implemented in section 3.3. However before going into details let us study the divergence (27) more quantitatively and consider the topological density correlation function.

3.2 $\langle q_0 q_x \rangle$ Correlation Function

In this section we consider one of the most important characteristics of the topological charge density distribution, namely, the correlation function $\langle q_0 q_x \rangle$. Note that the correlator $\langle q_0 q_x \rangle$ is known to be negative at any non-vanishing distance [13] provided that the definition of the topological density is local (see also Refs. [3, 4, 1] for discussions). However, the requirement of locality is *a priori* violated in HP¹ embedding approach so that $\langle q_0 q_x \rangle$, $|x| \neq 0$ is not obliged to be negative. We could only hope that the intrinsic non-locality is not so violent and extends up to some distance R_0 fixed in physical units. Note that this expectation is not completely groundless. Indeed, many non-perturbative observables, defined via HP¹ projection and studied in Refs. [9, 10], do not reveal any pathology and reproduce, in fact, the corresponding results in the full theory. Actually the degree of non-locality of HP¹ method could be estimated from the behavior of heavy quark potential measured at $a = 0.0601$ fm in [10], $R_0 \gtrsim 0.2$ fm. On the other hand, the investigation of $\langle q_0 q_x \rangle$ correlation function allows to find R_0 rather precisely and check its scaling properties.

Generically we expect that the correlator $\langle q_0 q_x \rangle$ is to be positive up to the distance R_0 and then should become negative provided that R_0 is finite. Remarkably enough these expectations are precisely confirmed by the measurements. The positive core of $\langle q_0 q_x \rangle$ correlation function at small $|x|$ is presented in physical units on Fig. 2. It is apparent that the points at various spacings are falling practically on the same curve with almost exponential $|x|$ -dependence

$$\langle q_0 q_x \rangle \propto e^{-|x|/R_{qq}}, \quad |x| \lesssim R_0. \quad (28)$$

Note that due to the logarithmic scale used on this plot the data sets are terminating at the same physical distance, for larger $|x|$ the correlation function becomes negative. Therefore the degree of non-locality inherent to HP¹ embedding method is

$$R_0 \approx 0.4 \text{ fm} \quad (29)$$

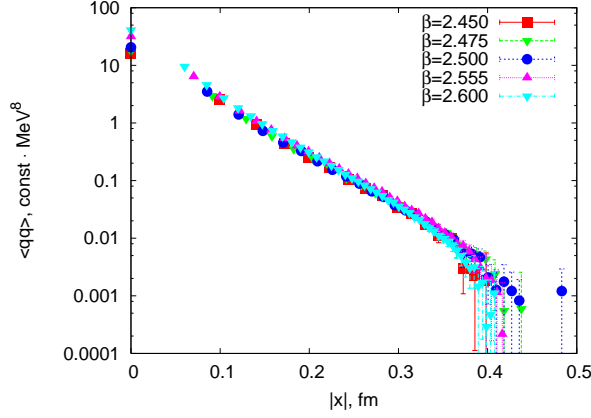


Figure 2: Positive core of topological density correlation function $\langle q_0 q_x \rangle$ at distances $|x| < R_0 \approx 0.4$ fm.

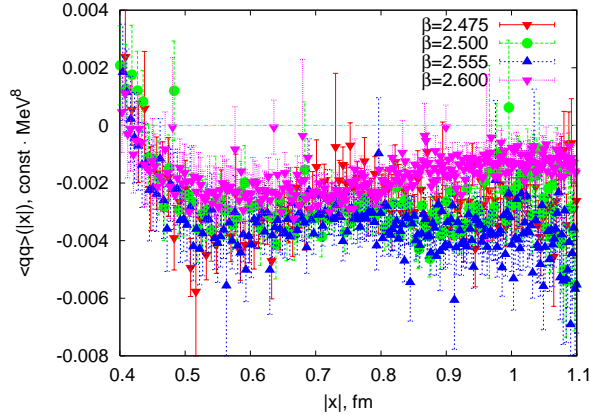


Figure 3: Negative part of the correlation function $\langle q_0 q_x \rangle$ at distances $|x| \geq R_0 = 0.4$ fm at various lattice spacings.

and is indeed constant in physical units as is evident from Fig. 2. Moreover, the almost perfect scaling of various data sets indicates once again that HP¹ projected fields do not contain any trace of the perturbation theory. Indeed, the mixture with perturbative contributions would lead to notable $\sim -1/|x|^8$ terms and would result in rather abrupt deviation from the exponential behavior. On the other hand, at large distances, $|x| \gtrsim R_0$, the correlation function $\langle q_0 q_x \rangle$ indeed becomes negative as is illustrated on Fig. 3. It is important that the negative part of $\langle q_0 q_x \rangle$ correlator does not show any singularity in the limit $a \rightarrow 0$, in particular, it has nothing to do with usual perturbative dependence.

Let us consider the scaling properties of the correlation length R_{qq} , Eq. (28). As might be evident already from Fig. 2, R_{qq} decreases with diminishing lattice spacing. In more details the dependence $R_{qq}(a)$ is presented on Fig. 4, from which it is apparent that the correlation length is likely to be linear function of a . In turn, all measured values of R_{qq} are less than even our finest lattice spacing resulting in rather small continuum value of the correlation length

$$R_{qq} = 0.0372(8) \text{ fm}, \quad (30)$$

which therefore should be considered heedfully. We could be only confident that R_{qq} is

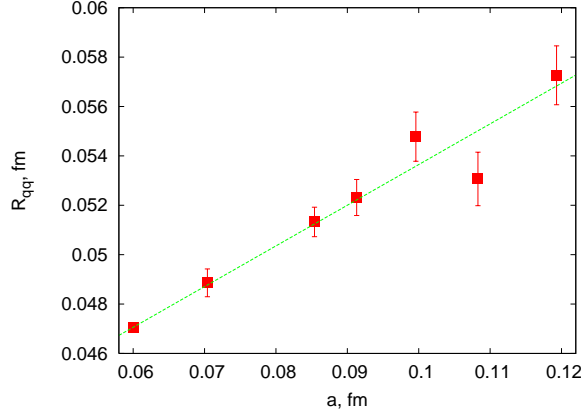


Figure 4: Correlation length R_{qq} , Eq. (28), as a function of lattice spacing. Line represents the best linear fit.

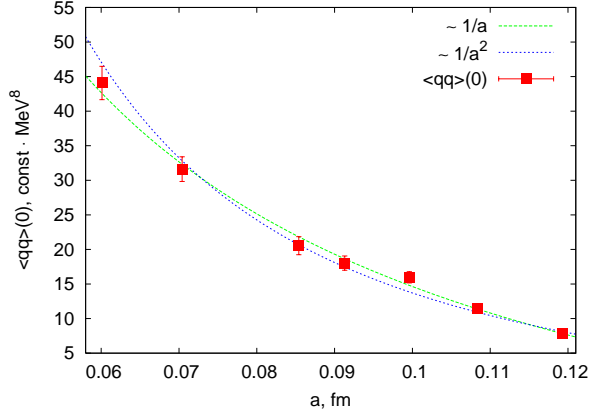


Figure 5: The mean squared topological density $\langle q^2 \rangle$ as a function of lattice spacing. Curves represent the best power law fits, Eq. (32).

of order of UV cutoff and indicates, in fact, that the topological charge sign-coherent regions are not four-dimensional. Indeed, this is the only possibility to reconcile rather large volume of most of the lumps with utterly small correlation length (30).

The factual absence of perturbative uncertainties in $\langle q_0 q_x \rangle$ correlation function implies that the limit

$$\langle q^2 \rangle = \lim_{|x| \rightarrow 0} \langle q_0 q_x \rangle \quad (31)$$

should be considered anew and that $\langle q^2 \rangle$ is not equivalent to pure contact term. Moreover, one could convince oneself that in the present case $\langle q^2 \rangle$ is indeed the appropriate definition of the characteristic topological density, $\bar{q}^2 = \langle q^2 \rangle$, and therefore it is crucial to consider its dependence upon the lattice spacing. The results of our measurements are presented on Fig. 5 and it is clear that $\langle q^2 \rangle$ indeed diverges in the continuum limit. However, it is important that this divergence has nothing in common with perturbatively expected $O(a^{-8})$ behavior, in fact, it is much weaker and is compatible only with linear or quadratic dependence

$$\langle q^2 \rangle = b_n + c_n \cdot a^{-n}, \quad n = 1, 2. \quad (32)$$

Unfortunately, our data points do not distinguish these power laws and are adequately described by either linear ($\chi^2_{n=1} = 0.9$) or quadratic ($\chi^2_{n=2} = 1.5$) one. Nevertheless, the ultraviolet divergence of characteristic topological density $\bar{q} \sim a^{-\alpha}$ within the HP¹ embedding method could be considered as firmly established. Moreover, we are confident that the corresponding power exponent is close to unity, $\alpha \lesssim 1$, and is in accord with theoretical expectations (13) and the estimate (27) obtained earlier.

3.3 Dimensionality of Topological Charge Fluctuations

In this section we introduce the method, which allows to investigate the dimensionality of the topological fluctuations without any additional parameters involved. Generically the idea is to consider some dynamical system the evolution of which is sensitive to the dimensionality of the ambient space. Then if we embed somehow this system into the topological density background, its evolution will reveal the effective number of available dimensions, which is to be naturally associated with the dimensionality of the relevant topological fluctuations. The simplest dynamical system of this sort could be constructed on the top of usual diffusion equation, which in turn is equivalent to propagation of random walks in the external environment. Correspondingly, the dimensionality D obtained this way is referred to as diffusion dimension. The purpose of this section is to precisely formulate and investigate this approach.

We start from the observation that the sole purpose of Λ_q is to separate the inevitably present noise (utterly small values of $q(x)$) in the topological density from the relevant fluctuations, which are associated with relatively large values of $q(x)$. Although the introduction of Λ_q indeed makes the notion of 'small' and 'large' well defined, the lumps geometry is strongly dependent upon the cut. It is apparent that the weak point of standard diffusion model is that the random walks are allowed to move freely regardless of the local magnitude of the topological density. We propose to modify the diffusion equation exactly at this point by allowing the random walk to move towards the regions of higher topological density with larger probability. In the language of the diffusion equation, which describes the propagation of heat, this amounts to the introduction of space-time dependent diffusion coefficient, which vanishes in the regions of small topological density. Hence heat is allowed to spread only within the domains of large $q(x)$. Then the decay rate of the initial heat pulse, which is the same as the return probability for corresponding biased random walk, reflects essentially the number of available dimensions within the relevant topological fluctuations and hence is to be identified with their dimensionality.

In fact, this general idea fixes almost uniquely the random walk model which replaces the simplest and well known diffusion equation. It is convenient to start directly from the microscopic rules of the biased random walk, which require that the probability $p(x, x + \mu)$ to move from x to the neighboring point $x + \mu$ is proportional to the magnitude of the topological density at final point

$$p(x, x + \mu) = \frac{1}{8\tilde{q}(x)} \cdot |q(x + \mu)|, \quad \tilde{q}(x) = \frac{1}{8} \sum_{\mu} (|q(x + \mu)| + |q(x - \mu)|). \quad (33)$$

Note that the use of the absolute value might look artificial, however, as will become clear in the moment, it indeed corresponds to generic situations.

It is straightforward to obtain the continuum diffusion-like equation which determines the probability $P(t, x)$ to reach the point x during the proper time interval t provided that the walker starts at $x = 0$ (see, e.g., Ref. [16])

$$\partial_t \Phi = \frac{1}{8q^2} \partial_x [q^2 \partial_x \Phi] , \quad \Phi(t, x) \equiv P(t, x)/q^2(x) , \quad (34)$$

where the initial condition is $P(0, x) = \delta(x)$. Note that q^2 here is due to the absolute value $|q|$ used in (33) and is to be replaced by q^{2n} if Eq. (33) involves $|q|^n$. Still Eq. (34) is not the usual diffusion equation, in particular, the decay rate of the initial perturbation (return probability in the random walk language) is not given by $P(t, 0) \propto t^{-D/2}$. To get the correct interpretation of (34) we introduce new coordinates $\zeta = \zeta(x)$ according to

$$\partial_\nu \zeta^\mu = q^2 \cdot \delta_\nu^\mu . \quad (35)$$

In the particular case of one dimensional problem (35) allows explicit solution $\zeta(x) = \int_{-\infty}^x q^2(y) dy$, where the fixed lower integration limit is taken generically at minus infinity. It is important that ζ is a single valued function of x almost everywhere, moreover, its range is determined by the magnitude of the topological density. Indeed, the regions of utterly small $q^2(x)$ are squeezed to almost one point by the map (35) regardless how large these regions were in x space. It is crucial that the term 'small' above obtains unambiguous and physically correct meaning of relative smallness since only the relative variation of the topological density does matter. Indeed, Eq. (34) is evidently scale invariant under $q^2 \rightarrow \lambda q^2$ and is equivalent to standard diffusion equation for everywhere constant $q(x)$. In terms of new coordinates Eq. (34) becomes the usual diffusion equation for $\Phi(t, \zeta)$

$$\partial_t \Phi = \frac{1}{8} \partial_\zeta [q^4 \partial_\zeta \Phi] . \quad (36)$$

We conclude therefore that the diffusion process (36) takes place in the regions of relatively large topological density and hence reflects properly the dimensionality of underlying topological background. Moreover, the decay rate of the initial perturbation is given by

$$\Phi(t, 0) \propto t^{-D/2} , \quad (37)$$

where D is the diffusion dimension of the relevant topological fluctuations.

The most straightforward way to find the dimensionality D numerically is to implement the random walk process the rules of which are completely specified by (33). The only subtlety here is the choice of the random walk starting point. Indeed, to improve the statistics it is desirable to consider

$$\Phi(t, \zeta) = \frac{\int d\zeta_0 \Phi(0, \zeta_0; t, \zeta_0 + \zeta)}{\int d\zeta_0} = \frac{\int dx_0 q^8(x_0) \Phi(0, x_0; t, x_0 + x)}{\int dx_0 q^8(x_0)} , \quad (38)$$

where $\Phi(0, \zeta_0; t, \zeta)$ is the probability to reach the point ζ during the time t starting at ζ_0 . Eq. (38) evidently means that the random walk starting point in x space is to taken with probability proportional to the eighth power of the topological density.

We measured the random walk return probability (36), (37) by first taking some random starting point, choosen with $\propto q^8$ probability, and considering in accord with (33)

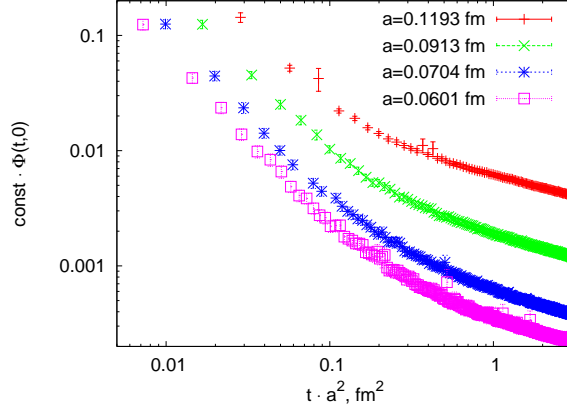


Figure 6: Return probability of modified random walk $\Phi(t, 0)$, Eqs. (36, 37), as a function of scaled proper time $t \cdot a^2$ at various spacings. Note that the curves start to bend at approximately the same point $R_0^2 \approx 0.2$ fm.

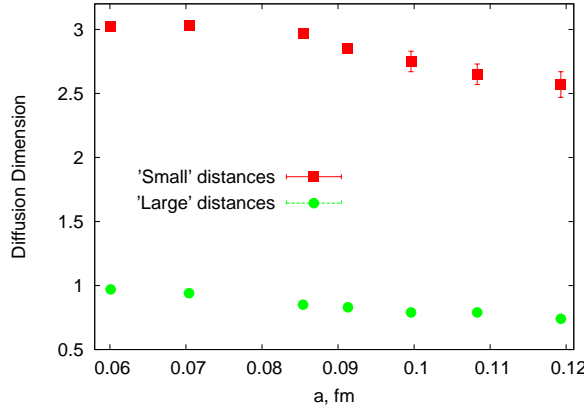


Figure 7: Scaling of the diffusion dimensions D , Eqs. (36, 37), obtained for 'small' $(\delta x)^2 \lesssim R_0^2$ and 'large' $(\delta x)^2 \gtrsim R_0^2$ random walks (see text).

the walk of total length $8 \cdot 10^3$. Then the quantity $\Phi(t, x) = P(t, x)/q^2(x)$ was constructed for each random walk and averaged with respect to $\approx V/2$ different starting points per each configuration. The results of our measurements of $\Phi(t, 0)$ are presented on Fig. 6, where for readability reasons not all available data sets are shown and $\Phi(t, 0)$ is normalized so that $\Phi(0, 0) = 1$. It is apparent that the dependence $\Phi(t, 0)$ is qualitatively similar to the case of usual pure random walk although there is indeed a notable difference. Namely, the return probability curves as a functions of rescaled proper time $t \cdot a^2$ on double-log plot of Fig. 6 bend quite notably at roughly the same point and are well described by the power law (37) at smaller and larger t . The bending starts at $\sqrt{t \cdot a^2} \approx 0.4 \div 0.5$ fm, which is very similar to the characteristic distance R_0 encountered already in section 3.2, and indicates that random walks propagating up to the distances $\delta x \lesssim R_0$ diffuse differently than ones probing larger scales $\delta x \gtrsim R_0$. In turn the effective dimensionality of topological fluctuations as is reflected by small and large scale walkers could be obtained by fitting the data at small and large δx to (37). The resulting small and large distance dimensionality as a function of lattice spacing is presented on Fig. 7. Remarkably enough even at small

distances the effective dimension is far from being 4. Instead in the continuum limit it seems to converge to the value

$$\lim_{a \rightarrow 0} D(a)|_{\delta x \lesssim R_0} = 3, \quad (39)$$

which is in full agreement with what had been discussed above. On the other hand, the random walks which are allowed to probe large distances behave effectively as in one dimension

$$\lim_{a \rightarrow 0} D(a)|_{\delta x \gtrsim R_0} = 1. \quad (40)$$

Note that Eqs. (39, 40) were obtained self-consistently and without any additional parameters involved. Taken at face value they indicate that the relevant vacuum topological fluctuations are three-dimensional lumps of characteristic transverse size of order $R_0 \approx 0.4$ fm. On the other hand, the lumps density is high enough to guarantee that they overlap along effectively one-dimensional submanifolds thus forming global percolating topological charge sign-coherent regions. Note that this picture is in complete agreement with both theoretical expectations and experimental data on the topological density. What is still to be considered is the internal consistency of this scenario, which is expressed by Eqs. (20), (22); this is the subject of the next section. However, at present we would not insist on the absolute validity of our conclusions since after all the diffusion dimension is only one possible definition of the dimensionality. It is still worth to confirm our findings with other methods.

3.4 Consistency Check

As was discussed in section 2.2 the crucial equations which relate the divergence of characteristic topological density \bar{q} and the dimensionality D of topological fluctuations are

$$\langle Q_+ Q_- \rangle = \langle Q_+ \rangle \langle Q_- \rangle, \quad (41)$$

$$\langle Q_\pm^2 \rangle - \langle Q_\pm \rangle^2 \propto \langle Q_\pm \rangle. \quad (42)$$

Moreover, their spacing independence (if confirmed by the data) allows to put rather stringent restrictions on both quantities. As far as the lattice measurements are concerned, Fig. 8 represents the ratios

$$\mathcal{A}(Q_\pm) = \frac{\langle Q_+ Q_- \rangle}{\langle Q_+ \rangle \langle Q_- \rangle} \quad (\text{circles}), \quad \mathcal{B}(Q_\pm) = \frac{\langle Q_\pm^2 \rangle - \langle Q_\pm \rangle^2}{\langle Q_\pm \rangle} \quad (\text{squares}), \quad (43)$$

as a functions of lattice spacing, where to improve the statistics the generic equalities $\langle Q_+^2 \rangle = \langle Q_-^2 \rangle$, $\langle Q_+ \rangle = \langle Q_- \rangle$ were used in calculation of $\mathcal{B}(Q_\pm)$. As is evident from that figure Eq. (41) is satisfied identically in the whole range of considered spacings while the proportionality coefficient entering Eq. (42) does not depend upon the lattice resolution well within numerical errors. Therefore the validity of Eq. (24) is firmly established. Then let us summarize the emerging qualitative picture of vacuum topological fluctuations which arises from the numerical data restricted by (24).

It is apparent that the most confidential data is available for the characteristic topological density. The theoretical arguments based on the existence of the quadratic correction

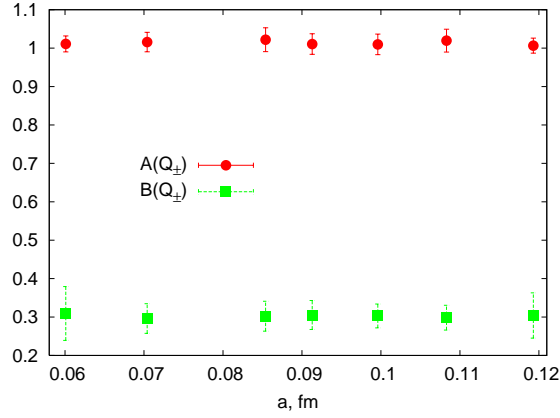


Figure 8: Fluctuations of the topological charges Q_{\pm} at various lattice spacings. Circles: spacing (in)dependence of the ratio $\mathcal{A}(Q_{\pm})$, Eq. (43); squares: the magnitude of Q_{\pm} relative fluctuations characterized by $\mathcal{B}(Q_{\pm})$, Eq. (43).

to the gluon condensate as well as numerical data obtained with various methods strongly suggest that the topological density is divergent at most linearly in the continuum limit

$$\bar{q} \sim a^{-\alpha}, \quad \alpha \lesssim 1. \quad (44)$$

Contrary to that the dimensionality of topological fluctuations is known much worse and is biased by theoretical uncertainties. Various estimations made both in this paper and in the literature [1, 2, 3, 4, 5] suggest that it is smaller or is of order three

$$\dim[V_{\pm}] \lesssim 3. \quad (45)$$

It is remarkable that Eqs. (44), (45) overlap only at one point consistent with Eq. (24)

$$\alpha = 1, \quad \dim[V_{\pm}] = 3. \quad (46)$$

Given that Eqs. (41), (42) are fulfilled with amazingly high accuracy we are forced to the conclusion that (46) is the only values consistent with both theoretical considerations and numerical data.

4 Conclusions

In this paper we further developed the $SU(2)$ gauge fields topology investigation method, based on the embedding of HP^1 σ -model into the given gauge background [9, 10]. Our prime purpose was to exploit the remarkable properties of HP^1 projected fields found in [10], namely, the factual absence of leading perturbative divergences and simultaneous existence of non-trivial quadratic power correction to gluon condensate. We argued that the explicitness of gauge fields topology in HP^1 embedding method leads to the conclusion that the non-perturbatively defined topological density is to be linearly divergent in the continuum limit. Note that this divergence has nothing to do with short distance perturbative singularities and is much weaker. The divergence of the topological density

by itself is almost academical problem since it is not directly observable. However, combined with the requirement of ultraviolet finiteness of topological susceptibility it leads to rather dramatic consequences for the geometry of relevant topological fluctuations. Namely, we argued that the topological charge is to be concentrated in three-dimensional submanifolds of four-dimensional Euclidean space. This is the only conclusion compatible with physical topological susceptibility, existence of the quadratic correction to the gluon condensate and which does not require the necessity to fine tune the Yang-Mills theory at UV scale. Moreover, the fine tuning assumption is testable and if we would insist that it is unnatural, then one could derive rather stringent relation between the divergence of the topological density and the dimensionality of submanifolds, which support the most of the topological charge. Note, however, that the lower dimensionality of topological fluctuations could also be considered as a sort of fine tuning, in which the explicit powers of UV cutoff are traded for unusual geometric properties. Qualitatively our results are in accord with modern trends in the literature, which discuss the lower dimensionality of physically relevant vacuum fluctuations [6, 8] and, in particular, of the topological density sign-coherent regions [1, 2, 3, 4, 5, 14].

The actual experimental verification of this scenario turned out to be rather intricate both conceptually and technically; we believe that all these problems were adequately addressed in our paper. The technical achievement is the development of fast and rather precise numerical algorithm of topological density evaluation, which allowed us to investigate the problem on the convincing statistical level. While the UV behavior of topological density could be studied directly, the dimensionality of relevant topological fluctuations is much more involved problem, which consists essentially in physical interpretation of the term 'relevant' above. We argued that the natural approach is to embed some dynamical system into the topological density background, the evolution of which is sensitive to the dimensionality of ambient space. The simplest system of this sort could be constructed on the top of usual random walk and the resulting definition of the topological regions dimensionality is defined uniquely, introduces no free parameters and is quite natural physics-wise.

As far as the results of numerical experiments are concerned, our data show unambiguously that non-perturbatively defined characteristic topological density is definitely divergent in the continuum limit. Moreover, we were able to obtain the upper bound on its leading spacing dependence. At the same time, the dimensionality of the relevant topological fluctuations was shown to be decidedly less than four albeit with large (mostly theoretical) uncertainties. Here the assumed absence of the fine tuning becomes crucial and we showed that it indeed does not happen. Instead the topological charges associated with sign-coherent regions fluctuate independently. We conclude therefore that the only possibility to satisfy all the restrictions is to have linearly divergent topological density distributed in three-dimensional domains.

Another notable result of our paper is the explicit demonstration of finite degree of non-locality inherent to HP¹ embedding approach. We argued that the method is non-local only up to the distances of order $R_0 \approx 0.4$ fm, which is indeed constant in physical units. Finally we note that our results, although being in accord with the existing literature, still require an independent confirmation, in particular, with respect to the definition of dimensionality of the topological charge sign-coherent regions.

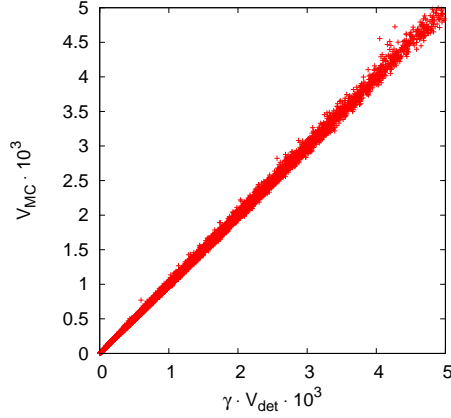


Figure 9: Cumulative distribution of $V_{MC}(T)$ and $V_{det}(T)$ (see text).

Acknowledgments

The authors are grateful to Prof. V.I.Zakharov and to the members of ITEP lattice group for stimulating discussions. The work was partially supported by grants RFBR-05-02-16306a and RFBR-05-02-17642. F.V.G. was partially supported by INTAS YS grant 04-83-3943.

Appendix

Here we describe in details the numerical algorithm used in this paper to calculate the topological charge density. The general formulation of the problem could be found in Refs. [9, 10]. Essentially it reduces to the evaluation of the volume $V(T)$ of 4-dimensional spherical tetrahedron T embedded into S^4 with vertices n_i^A given in terms of five $i = 0, \dots, 4$ unit five-dimensional $A = 0, \dots, 4$ vectors, $(\vec{n}_i)^2 = 1$.

It is clear that for near vanishing $V(T)$ the volume is given by $V(T) = \det_{Ai}[n_i^A]$. Thus the volume of finite tetrahedron could be found by triangulating it into the set of small tetrahedra and summing up the infinitesimal volumes. In fact, our method works recursively until the determinant estimation of the volume of input tetrahedron is larger than 10^{-6} ; this way we indeed obtain the optimal performance. However, the determinant-based volume estimation is reliable and uniform only if the angles between all input vertices are small enough, e.g. $(\vec{n}_i, \vec{n}_j) > 0$. In this case it suffices to place new triangulation vertex at $\vec{m} \propto \sum_i \vec{n}_i$ and complete the recursion cycle. However, this procedure must be modified if there are at least two input vertices i and j for which $(\vec{n}_i, \vec{n}_j) < 0$. Indeed, in this case the above recursions converge non-uniformly and eventually lead to almost degenerate tetrahedra with large volume but still almost vanishing determinant. The needed modification is to take the new vertex at $\vec{m} \propto \vec{n}_i + \vec{n}_j$ which guarantees that eventually we will get $(\vec{n}_i, \vec{n}_j) > 0 \forall i, j$.

Let us note that for given accuracy of the determinant volume estimation for small tetrahedra (which is 10^{-6} in our case) the volume of the original tetrahedron is evaluated, in fact, with finite bias which is due to the sphericity of every small tetrahedron. However for small enough volumes the sphericity could be accounted for by simple rescaling of

the determinant estimation. To calibrate the present algorithm we compared it with our previous Monte-Carlo based method. To this end we generated $5 \cdot 10^4$ random spherical tetrahedra and applied both algorithms to each of them thus obtaining Monte-Carlo $V_{MC}(T)$ and determinant-based $V_{det}(T)$ volume estimations. Fig. 9 represents the cumulative distribution of $V_{MC}(T)$, $V_{det}(T)$, which turns out to be astonishingly narrow and is fairly compatible with linear dependence

$$V_{MC}(T) = \gamma \cdot V_{det}(T), \quad \gamma = 1.1285(5), \quad (\text{A.1})$$

where the optimal value of γ coefficient results from the best linear fit. Note that the plot on Fig. 9 is restricted to $V(T) \lesssim 5 \cdot 10^{-3}$, which is far beyond the maximal value of topological density even for our largest spacing; however, the linear dependence (A.1) remains valid even at larger $V(T)$. Thus we are confident that the new triangulation method is definitely compatible with old Monte-Carlo approach in the relevant range of lattice spacings.

Finally, we performed the same check as one described in [10]. Namely, we confronted the global topological charge, which could be found unambiguously for each our configuration with one calculated with present algorithm. It turns out that they agree in all cases with no exceptions. Moreover, we found that the determinant-based algorithm gives even narrower distribution of Q_{float} around integer numbers compared to that of old Monte-Carlo based approach. We conclude therefore that the new method of the topological density calculation is superior to the old one both in accuracy and performance.

References

- [1] I. Horvath *et al.*, Phys. Rev. D **68**, 114505 (2003) [arXiv:hep-lat/0302009]; Nucl. Phys. Proc. Suppl. **129**, 677 (2004) [arXiv:hep-lat/0308029]; Phys. Lett. B **612**, 21 (2005) [arXiv:hep-lat/0501025];
I. Horvath, Nucl. Phys. B **710**, 464 (2005) [Erratum-ibid. B **714**, 175 (2005)] [arXiv:hep-lat/0410046];
A. Alexandru, I. Horvath and J. b. Zhang, Phys. Rev. D **72**, 034506 (2005) [arXiv:hep-lat/0506018].
- [2] C. Gattringer, M. Gockeler, P. E. L. Rakow, S. Schaefer and A. Schafer, Nucl. Phys. B **617**, 101 (2001) [arXiv:hep-lat/0107016];
C. Aubin *et al.* [MILC Collaboration], Nucl. Phys. Proc. Suppl. **140**, 626 (2005) [arXiv:hep-lat/0410024];
C. Bernard *et al.*, PoS **LAT2005**, 299 (2005) [arXiv:hep-lat/0510025].
- [3] Y. Koma, E. M. Ilgenfritz, K. Koller, G. Schierholz, T. Streuer and V. Weinberg, PoS **LAT2005**, 300 (2005) [arXiv:hep-lat/0509164];
E. M. Ilgenfritz, K. Koller, Y. Koma, G. Schierholz, T. Streuer and V. Weinberg, arXiv:hep-lat/0512005.
- [4] I. Horvath *et al.*, Phys. Lett. B **617**, 49 (2005) [arXiv:hep-lat/0504005].

- [5] F. V. Gubarev, S. M. Morozov, M. I. Polikarpov and V. I. Zakharov, JETP Letters **82**, 381 (2005) [arXiv:hep-lat/0505016]; PoS **LAT2005**, 143 (2005) [arXiv:hep-lat/0510098].
- [6] M. I. Polikarpov, S. N. Syritsyn and V. I. Zakharov, JETP Lett. **81**, 143 (2005) [Pisma Zh. Eksp. Teor. Fiz. **81**, 177 (2005)] [arXiv:hep-lat/0402018];
A. V. Kovalenko, M. I. Polikarpov, S. N. Syritsyn and V. I. Zakharov, Phys. Lett. B **613**, 52 (2005) [arXiv:hep-lat/0408014]; PoS **LAT2005**, 328 (2005) [arXiv:hep-lat/0510020].
- [7] V. G. Bornyakov, M. N. Chernodub, F. V. Gubarev, M. I. Polikarpov, T. Suzuki, A. I. Veselov and V. I. Zakharov, Phys. Lett. B **537**, 291 (2002) [arXiv:hep-lat/0103032];
M. N. Chernodub and V. I. Zakharov, Nucl. Phys. B **669**, 233 (2003) [arXiv:hep-th/0211267];
V. G. Bornyakov, P. Y. Boyko, M. I. Polikarpov and V. I. Zakharov, Nucl. Phys. B **672**, 222 (2003) [arXiv:hep-lat/0305021];
V. I. Zakharov, Nucl. Phys. Proc. Suppl. **121**, 325 (2003); arXiv:hep-ph/0312210;
V. G. Bornyakov, P. Y. Boyko, M. I. Polikarpov and V. I. Zakharov, Nucl. Phys. Proc. Suppl. **129**, 668 (2004) [arXiv:hep-lat/0309021];
A. V. Kovalenko, M. I. Polikarpov, S. N. Syritsyn and V. I. Zakharov, Phys. Rev. D **71**, 054511 (2005) [arXiv:hep-lat/0402017].
- [8] F. V. Gubarev, A. V. Kovalenko, M. I. Polikarpov, S. N. Syritsyn and V. I. Zakharov, Phys. Lett. B **574**, 136 (2003) [arXiv:hep-lat/0212003];
V. I. Zakharov, arXiv:hep-ph/0306261; arXiv:hep-ph/0306262; arXiv:hep-ph/0309178;
V. I. Zakharov, Phys. Usp. **47**, 37 (2004) [Usp. Fiz. Nauk **47**, 39 (2004)];
V. I. Zakharov, arXiv:hep-ph/0309301; Phys. Atom. Nucl. **68**, 573 (2005) [Yad. Fiz. **68**, 603 (2005)] [arXiv:hep-ph/0410034];
V. I. Zakharov, AIP Conf. Proc. **756**, 182 (2005) [arXiv:hep-ph/0501011].
- [9] F. V. Gubarev and S. M. Morozov, Phys. Rev. D **72**, 076008 (2005) [arXiv:hep-lat/0509011].
- [10] P. Y. Boyko, F. V. Gubarev and S. M. Morozov, '*SU(2) gluodynamics and HP¹ σ -model embedding: scaling, topology and confinement*', arXiv:hep-lat/0511050.
- [11] E. M. Ilgenfritz, Y. Koma, G. Schierholz, T. Streuer and V. Weinberg, talk given at the '*Workshop on Computational Hadron Physics*', Nicosia, Cyprus, September 14-17, 2005 (unpublished).
- [12] P. E. L. Rakow, PoS **LAT2005**, 284 (2005) [arXiv:hep-lat/0510046].
- [13] E. Seiler, Phys. Lett. B **525**, 355 (2002) [arXiv:hep-th/0111125];
M. Aguado and E. Seiler, Phys. Rev. D **72**, 094502 (2005) [arXiv:hep-lat/0503015].
- [14] A. V. Kovalenko, S. M. Morozov, M. I. Polikarpov and V. I. Zakharov, arXiv:hep-lat/0512036.

- [15] J. Fingberg, U. M. Heller and F. Karsch, Nucl. Phys. B **392**, 493 (1993);
G. S. Bali, K. Schilling and A. Wachter, Phys. Rev. D **55**, 5309 (1997);
G. S. Bali, K. Schilling and C. Schlichter, Phys. Rev. D **51**, 5165 (1995);
B. Lucini and M. Teper, JHEP **0106**, 050 (2001).
- [16] C. Itzykson, J. -M. Drouffe, *“Statistical Field Theory”*, Cambridge Univ. Press, 1989.